

**A PRELIMINARY STUDY OF  
STATIONARY SHOCK-INDUCED COMBUSTION  
WITH HYDROGEN-AIR MIXTURES**

By

**R. P. Rhodes and D. E. Chriss**  
RTF, ARO, Inc.

July 1961

PROPERTY OF U. S. AIR FORCE  
AEDC LIBRARY  
IF AVAILABLE

**ARNOLD ENGINEERING  
DEVELOPMENT CENTER**

**AIR FORCE SYSTEMS COMMAND**



Property of U. S. Air Force  
AEDC LIBRARY  
F40600-74-C-0001

A PRELIMINARY STUDY OF  
STATIONARY SHOCK-INDUCED COMBUSTION  
WITH HYDROGEN-AIR MIXTURES

By

R. P. Rhodes and D. E. Chriss  
RTF, ARO, Inc.

July 1961

ARO Project No. 150067  
ARDC Program Area 801A, AFOSR Project 9751, Task 37510

Contract No. AF 40(600)-800 S/A 24(61-73)

**ABSTRACT**

A study of the shock-induced combustion of hydrogen-air mixtures was made in a small Mach number 3 wind tunnel at a total pressure level of 45 psia. Combustion was induced by a normal shock wave which resulted from the interaction of two oblique shock waves produced by wedges on the tunnel walls. Significantly different phenomena were observed when the fuel injector was moved from the subsonic portion of the nozzle into the throat. With fuel injection in the throat, ignition denoted by emission glow from the sodium introduced with the hydrogen did not occur until some distance downstream of the normal shock wave. Some data are presented showing this delay as a function of the static temperature behind the shock wave.

## CONTENTS

	<u>Page</u>
ABSTRACT . . . . .	3
NOMENCLATURE . . . . .	7
INTRODUCTION . . . . .	9
APPARATUS . . . . .	10
PROCEDURE . . . . .	12
RESULTS AND DISCUSSION . . . . .	12
CONCLUDING REMARKS . . . . .	19
REFERENCES . . . . .	20

## ILLUSTRATIONS

Figure

1. Supersonic Combustion Tunnel	
a. Photograph . . . . .	21
b. Schematic . . . . .	21
2. Upstream Fuel Injector Installation . . . . .	22
3. Throat Fuel Injector Installation . . . . .	23
4. Test Section Temperature, Pressure, and Sampling Probe Design . . . . .	24
5. Wedge-Type Pressure Probe . . . . .	25
6. Sodium Hydroxide Vaporizer . . . . .	26
7. Plenum Periscope Installation . . . . .	27
8. Typical Views through the Plenum Periscope . . .	28
9. Test Section Schlieren Photograph	
a. No Fuel Injection, No Reaction, $T_{T0} = 1460^{\circ}\text{R}$ . . . . .	29
b. Emission with Upstream Injector, $T_{T0} = 1460^{\circ}\text{R}$ , Maximum $\text{H}_2$ Concentration 0.08 mole $\text{H}_2$ /mole Air. . . . .	30
c. Emission with Throat Injection, $T_{T0} = 2000^{\circ}\text{R}$ , Maximum $\text{H}_2$ Concentration 0.08 mole $\text{H}_2$ /mole Air. . . . .	31
10. Test Section Hydrogen Concentration	
a. Upstream Fuel Injector . . . . .	32
b. Throat Fuel Injector . . . . .	33

FigurePage

11.	Effect of Test Section Centerline Total Temperature Ratio from Burning Hydrogen	
a.	On Tunnel Throat Pressure Ratio . . . . .	34
b.	On Test Section Centerline Free-Stream Total Pressure Ratio . . . . .	35
c.	On Test Section Centerline Free-Stream Mach Number . . . . .	36
d.	On Test Section Centerline Indicated Total Pressure Ratio . . . . .	37
12.	Ignition Delay in the SCT	
a.	As a Function of Temperature and Oxygen Concentration . . . . .	38
b.	As a Function of Temperature . . . . .	39

## NOMENCLATURE

$M_1$	Test section Mach number ahead of normal shock wave
$M_2$	Test section Mach number behind normal shock wave
$P_{throat}$	Throat static pressure
$P_T$	Test section total pressure ahead of normal shock wave
$P_{T_0}$	Plenum chamber total pressure downstream of preheater
$P_{T'}$	Test section total pressure behind normal shock wave
$R$	Ideal gas constant, $ft^2/sec^2-^{\circ}R$
$T_T$	Test section total temperature, $^{\circ}R$
$T_{T_0}$	Test section total temperature, preheater only, $^{\circ}R$
$T$	Test section static temperature, $^{\circ}R$
$V_2$	Velocity downstream of the normal shock wave
$NO_2[C]$	Oxygen content, moles/cc
$\gamma$	Ratio of specific heats
$\tau$	Ignition delay time, sec

## INTRODUCTION

The first experimental investigation of shock-induced combustion in a supersonic stream with a stationary shock wave was conducted between 1957 and 1959 by Gross (Ref. 1) at Fairchild Engine Division and by Nicholls (Ref. 2) at the University of Michigan.

Shock-induced combustion occurs when a combustible mixture is rapidly heated to above its ignition temperature by a shock wave. The combustion reaction becomes detectable after a delay which is determined by the rates of the initiating reactions. Experimentally, this combustion reaction can be produced by introducing fuel near the throat of a supersonic tunnel in such a manner that ignition does not occur at the injector; then the combustible mixture which is formed flows through the nozzle and across a normal shock wave which is formed in a free jet from a highly underexpanded nozzle or by the interaction of oblique shocks formed by wedges at the wall of the nozzle. This combustion phenomenon differs from classical detonation waves in at least one important way: shock-induced combustion occurs in a flowing stream where a shock wave exists independent of the combustion wave; in the case of classical detonation the shock is formed by the pressure rise caused by the combustion. Since the existence of the shock wave is not dependent on the combustion, shock-induced combustion can exist over a wide range of heat release for a given Mach number while classical detonations have experimentally been limited to a definite Mach number for a given heat release.

The results of the work conducted by Gross (Ref. 1) disagreed in several major respects from those obtained by Nicholls (Ref. 2). The areas of disagreement were (1) the delay between the shock wave and the start of rapid burning which Nicholls found to be an exponential function of temperature and Gross did not observe, (2) the "hysteresis effect", in which shock-induced combustion is stable below the temperature necessary to ignite it, which Gross observed in all cases and Nicholls did not find, and (3) the upstream movement of the normal shock with increasing heat release, which Gross found and Nicholls was unable to detect except in a very few cases at high heat release rates.

The most significant of these differences was the "hysteresis effect", since, if hysteresis does in fact exist, it implies that heat is transferred forward from the combustion

zone so that the incoming gas is heated by the reaction; a lack of hysteresis implies that transport effects upstream of the combustion zone are negligible.

The study of shock-induced combustion waves at the Rocket Test Facility (RTF) of the Arnold Center (AFSC)\* was begun in March 1960 using the supersonic combustion tunnel (SCT) (Ref. 3). This report describes and discusses the experiments made to examine the phenomena observed by Gross in this same experimental apparatus and the attempt to reproduce in a confined flow the phenomena which were observed by Nicholls in a free jet flow.

## APPARATUS

### SUPERSONIC COMBUSTION TUNNEL

A detailed description of the supersonic combustion tunnel which was used by Gross for his work at Fairchild and for these tests is presented in Ref. 3. A schematic layout of the tunnel and a photograph of the nozzle and test section are shown in Fig. 1. Air, which may be preheated by an indirect-fired heater up to 1200°F, enters the plenum where it can be further heated to a maximum of 2500°F by the combustion of hydrogen. The nozzle is two-dimensional, having an exit area of 3 in. wide by 5 in. high and producing a test section Mach number of 3.1. The test section contains wedges which are located on the top and bottom walls and which produce a pair of oblique shocks and a connecting normal shock. This normal shock is used to stabilize the combustion. The test section also contains two pairs of ports which may be used for windows or for mounting instrumentation. A diffuser is located behind the test section to reduce pressure loss. The test fuel is preheated to about 700°F by a heater in the inlet ducting.

### FUEL INJECTORS

Two fuel injectors were used. The first, designated the upstream fuel injector, was used by Gross in his work with the SCT. The fuel injection plane is located about one inch upstream of the geometric throat of the tunnel where the Mach number is about 0.6. The design of this injector and its location in the tunnel are shown in Fig. 2. The second fuel injector, the throat injector, is a thin airfoil section with the injector tube trailing aft on the centerline of the tunnel and discharging near the geometric throat of the tunnel. The design of this injector and its location are shown in Fig. 3.

---

\*Air Force Systems Command



## INSTRUMENTATION

All temperatures were measured with chromel-alumel thermocouples and recorded on a recording potentiometer. The test section total temperature and total pressure were measured with a combination probe which could be used either for temperature or pressure measurement or for gas sampling. A sketch of the probe tip design and a schematic layout of the pressure-temperature and sampling hookup is shown in Fig. 4.

All air pressures were measured with a 120-in. mercury-filled manometer board and recorded photographically. Hydrogen pressures were measured with transducers and recorded manually. The shock position, the test section probe position, and the location of emission from high temperature zones were determined by photographing the test section with the schlieren camera using a combination of collimated light from the schlieren light source and direct emission from the test section.

The local concentration of hydrogen in the test section was measured by drawing a sample of gas through the test section probe into a thermal conductivity cell which contained four platinum resistance elements connected in a bridge circuit. A bridge voltage was selected which kept the bridge wires below the temperature where catalytic combustion would be expected. The output of the bridge was read on a recording potentiometer. The instrument was calibrated with hydrogen-air mixtures of known composition which were drawn from a container through the sampling system.

A wedge-type probe consisting of a 10-deg half angle wedge, one inch wide, was used to measure Mach number and total pressure in the test section (Fig. 5). A static tap was located on one face of the wedge, and a total pressure tube was placed parallel to the wedge surface on the same side. The total temperature was measured with a chromel-alumel self-aspirating thermocouple which also served to support the wedge.

## SODIUM INJECTION

Since nearly all the emission from a hydrogen-air flame comes from ultraviolet and infrared band spectra, it was necessary to add a contaminant which would radiate in the visible portion of the spectrum. Sodium hydroxide was chosen because of its availability, the bright emission from the sodium D line, and because of the relatively high volatility of this compound. The device for introducing the sodium is shown in Fig. 6. A current of about 25 amp at about 3 volts

flowed through the sodium hydroxide after the device was preheated to about 500°F by flowing heated hydrogen through it. This current either vaporized or electrolyzed the molten sodium hydroxide. The amount of sodium added to the stream could be controlled by varying the voltage with a rheostat. After this device had been in operation for some time the lines downstream became contaminated, and the sodium emission was seen in the flame even when the vaporizer was turned off. When too much contamination occurred, it was necessary to clean the system before any control of the brightness of the flame could be obtained.

### PROCEDURE

The inlet air temperature was brought to 1000°F using the indirect-fired heater. During the heat-up, the plenum (Fig. 1b) total pressure was maintained at about 50 psia, and the air was discharged through the test section to atmosphere. When the desired temperature was reached, supersonic flow in the test section was established by reducing the diffuser exit pressure with the RTF exhaust system.

The desired fuel flow was then established, and the inlet temperature was increased using the plenum heater until ignition occurred. Ignition was detected by an abrupt rise in test section temperature. The desired plenum temperature was then set, and the data were recorded.

For all runs the inlet air was dried by chemical driers. However, when the plenum heater was used, the moisture content increased, and the oxygen content decreased as the temperature was raised.

### RESULTS AND DISCUSSION

The study of shock-induced combustion was undertaken to obtain information which would define the aerodynamics and thermochemistry of the process. The most likely cause of the differences between the work of Gross and Nicholls was that burning occurred at the fuel injector in the case of the configuration used by Gross. If the hydrogen were burning in the wake of the injector strut, this combustion would blow out at a lower temperature than the ignition temperature, and any phenomena in the test section which resulted from this combustion would appear to show a hysteresis. Burning behind the injector would also reduce the delay of reignition at the shock wave of any remaining fuel by increasing the static temperature and possibly by providing a

source of free radicals which had not had time to recombine. Burning upstream of the shock would also explain the change in shock wave position with fuel flow.

The first part of this investigation was designed to determine whether or not burning existed behind the upstream fuel injector and if so, what percentage of the combustion was completed upstream of the shock wave. The second part was designed to produce data showing the effect of test section temperature on the ignition, denoted by the start of sodium emission from the reaction zone, which did not occur until some distance downstream of the normal shock wave for a case in which combustion at the fuel injector was known to be absent.

## COMPARISON OF THE PHENOMENA OBTAINED WITH TWO FUEL INJECTORS

### Observation of the Throat Area

In an attempt to determine whether combustion was occurring in the region of the upstream fuel injector, a small periscope was installed in the plenum of the supersonic combustion tunnel. A view (looking down on the tunnel) showing this installation is presented in Fig. 7. The quality of the prism used in the periscope was poor, but sufficient resolution was obtained so that it was possible to locate the nozzle throat and the hydrogen injector on the photographs. The probe in the test section was used to verify ignition and was then removed to prevent its incandescent glow from showing in the field of the periscope.

Typical frames from motion pictures taken through the periscope showing the upstream injector are presented in Fig. 8. An examination of individual frames shows a flame near the tip of the injector. The lack of symmetry of the flame as seen in the photograph is caused by the angle of view rather than by any inherent lack of symmetry in the system.

When the throat injector was used to introduce the hydrogen, a visual observation through the periscope showed no evidence of burning near the fuel injector.

### Observation of the Test Section

A number of photographs (Fig. 9) of the phenomena in the test section were taken with schlieren and by direct emission. Sodium was added to the hydrogen in the form of sodium hydroxide which was vaporized into the fuel just upstream of the hydrogen injector (see APPARATUS). The

photographs were made by exposing the film for about 1/50 sec with the schlieren light on and the knife edge adjusted to give a dark field with bright shock waves and then for about 30 sec with the schlieren light off. Since the test section was in focus on the film in the schlieren system, the exposure with the schlieren light off gave a photograph in the light emitted by the flame.

A schlieren photograph of the test section with supersonic flow established but without hydrogen flow is shown in Fig. 9a. The oblique shock waves, which appear to be quite straight, originate slightly ahead of the intersection of the wedge and the tunnel wall because of the boundary layer on the nozzle blocks.

A combination schlieren and emission photograph (Fig. 9b) of the phenomena which occurred when the upstream injector was used shows a number of interesting features. First, there is emission from sodium upstream of the normal shock. If there were no such upstream burning, the static temperature upstream of the shock wave would be about  $500^{\circ}\text{R}$  for a total temperature of  $1460^{\circ}\text{R}$ . Since  $500^{\circ}\text{R}$  is too low to produce thermal emission from the sodium atoms, there must be heat addition upstream of the shock.

Second, there is a distinct curvature of the oblique shocks toward the incoming gas in the region where the sodium emission indicates that the gas is heated. If it may be assumed that the turning angle behind the shock is constant, then this increase in shock angle must reflect a decrease in Mach number in the heated portion of the stream. A reduction in Mach number would be expected if heat were added in the supersonic stream or if heat addition near the throat caused the sonic line to move downstream, which would reduce the effective expansion ratio of the nozzle. In a shock wave system consisting of a normal shock connecting two oblique shocks, though no quantitative calculations can be made defining the point at which the normal shock occurs, it is qualitatively known that for a given wedge angle the normal shock moves upstream as the Mach number is decreased, and the oblique shock angle increases. Thus a reduction in Mach number in the core upstream of the normal shock could also explain the forward movement of the shock with increased heat release (see Figs. 9a and b).

When the throat fuel injector was used, the observed phenomenon was like that shown in Fig. 9c. There was no appreciable movement of the normal shock, and sodium emission from the combustion zone might be seen after a short delay.

The fuel distribution for the two fuel injectors, measured about one inch ahead of the normal shock position, without combustion, and at a total temperature of  $1460^{\circ}\text{R}$ , is shown in Fig. 10. The area covered by hydrogen is slightly larger in the case of the upstream injector, probably because of the turbulence from the wake of this injection strut. In the case of the upstream injector (Fig. 9b), the emission comes from an area which is about the same size as that containing fuel. With the throat injector (Fig. 9c), however, the combustion is limited to the area behind the normal shock wave, an indication that this is the only place where the static temperature is high enough to cause ignition.

#### Pressure Variations with Combustion

As a further check on combustion behind the injector, pressure measurements were taken in the plenum, throat, and test section during the combustion process. It would be desirable to present these pressure data as a function of heat release or fuel flow, but it would be quite difficult and time consuming to measure the hydrogen concentration for each data point. Also, these hydrogen concentrations must be measured when the total temperature is below the ignition temperature or the gas will burn at the sampling probe, and therefore, it would be necessary to assume that the hydrogen distribution is independent of temperature level. Another difficulty with using the hydrogen concentration to correlate pressure effects is the fact that these effects should be a function of heat addition rather than of gas flow and that to use the hydrogen concentration implies 100-percent combustion efficiency, which may not exist. For these reasons,  $T_T/T_{T_0}$ , the ratio of total temperature on the test section centerline with and without fuel flow, has been used to correlate the effect of combustion on pressure.

The test section centerline stagnation temperature,  $T_{T_0}$ , was the same as the plenum centerline temperature within about two percent when there was no preheating in the plenum. When the preheater was used there was a continuous mixing of the hot core from the centrally located preheater burner with the cooler boundary flow, and an axial temperature gradient existed from the plenum to the test section. The test section centerline temperature was about  $400^{\circ}\text{F}$  lower than the plenum core at a  $T_{T_0}$  of  $2200^{\circ}\text{R}$ .

Throat Pressure Variation - The effect of the temperature rise ratio on the ratio of the static pressure in the throat to the total pressure in the plenum is shown in Fig. 11a. When the upstream hydrogen injector was used, an

increase in test section temperature ratio produced an increase in the pressure ratio, an indication that at least some of the combustion was taking place between the injector and the throat. There was no change in the pressure ratio when hydrogen was injected and the air temperature was too low for ignition to occur.

When the throat injector was used, there was no change in the throat pressure ratio as hydrogen was introduced. The smaller range of  $T_T/T_{T_0}$  for the throat injector resulted from the larger values of  $T_{T_0}$  used and the limitation of the maximum  $T_T$  which could be measured with the probe.

With either injector there was a small change in throat pressure ratio as the plenum temperature was increased. This was probably caused by the change in the ratio of specific heats of the gas entering the nozzle. There was also a small difference between the pressures measured with the two injectors. This difference may be the result of flow disturbances around the injectors themselves since the throat static taps were located in the region of the wake from the fuel injectors.

Test Section Pressure and Mach Number Variation - The test section pressures and Mach numbers obtained using the upstream fuel injector were measured with a wedge mounted in the test section (Fig. 5). The data obtained were the static pressure on the wedge, the indicated total pressure above the wedge surface behind the oblique shock wave, and the total temperature. The Mach number along the wedge behind the oblique shock was calculated from the ratio of the static pressure on the wedge to the indicated total pressure behind the oblique shock wave. This Mach number and the wedge angle measured from schlieren photographs were used to calculate the free-stream Mach number and total pressure using oblique shock wave functions and the ratio of specific heats calculated at the total temperature of the stream. The calculations were made assuming that there was no total temperature change across the shock wave from the wedge. The results of these measurements are shown in Figs. 11b and c. Both the centerline Mach number and the centerline total pressure decreased as the temperature was raised by the burning hydrogen.

The experimental ratio of the total pressure behind the normal shock to the plenum pressure is compared in Fig. 11d with the theoretical total pressure ratio in a one-dimensional hydrogen air detonation at Mach 3.1. The data were obtained using the upstream fuel injector and at

a  $T_{T0}$  of  $1460^{\circ}\text{R}$ ; the theoretical pressure ratio was obtained from data presented by Gross (Ref. 1) for the same initial temperature. The experimental total pressure loss was much larger than would be expected from a one-dimensional detonation. Part of the data on this curve was obtained by direct measurement of the total pressure behind a normal shock wave in the test section, and part was calculated from pressure data taken on the wedge. Although the measured and calculated values cover a different range of  $T_T/T_{T0}$ , both sets of data fall on a single smooth curve.

The test section pressures and Mach numbers calculated from the data taken on the instrumentation wedge are subject to question depending on the validity of the assumption that no reaction took place behind the oblique shock from the wedge or behind the normal shock on the total pressure tube. There are two factors which tend to show that this assumption is valid. First, there was a distinct curvature of the oblique shock waves toward the incoming flow when combustion was taking place upstream (Fig. 9b), and the calculated change in Mach number based on the wedge data is of the order of magnitude necessary to cause the observed change in shock wave angle. Second, the fact that the same values of  $P_T'/P_{T0}$  were obtained from direct measurements with a total pressure tube as were calculated from pressure data taken on the wedge-type pressure probe, assuming no reaction on the wedge, (Fig. 10d) gives strong support to the validity of the assumption.

With the throat injector, no comparable pressure data (Figs. 11b, c, and d) could be obtained in the test section. When the test section temperature was high enough to cause ignition behind a normal shock wave, the hydrogen ignited behind the normal shock on the tip of the probe, and the free-stream total pressure could not be calculated using adiabatic normal shock relationships.

All the phenomena seen in the test section when the upstream injector was used to introduce fuel can be explained as the result of combustion near the injector. The large reduction of the test section centerline Mach number and the total pressure indicated by the data from the wedge-type probe can only be explained if a large amount of heat had been released upstream of the probe. There is insufficient information to calculate the degree of completion, but there is no evidence to indicate that the reaction is not essentially complete upstream of the test section.

## IGNITION DELAY MEASUREMENTS

A series of experiments were made to study the phenomena which occurred in the test section when the throat injector was used and no combustion occurred upstream of the normal shock wave. When the fuel flow was set and the test section temperature was increased from about 1000°F using the pre-heater, no change was evident in the test section until a temperature of about 1750°R, indicated by the test section thermocouple, was reached. At this point glow from the sodium in the fuel could be seen behind the shock (Fig. 9c). As the temperature was raised further, the glow brightened and its upstream edge moved toward the normal shock. At no time was there any appreciable movement of the normal shock or any evidence of burning upstream of the normal shock. Figure 9c is a combination schlieren and emission photograph of the test section showing this phenomena. The ignition delay time was calculated for several fuel flows and at various test section temperatures by measuring the distance between the normal shock and the beginning of emission from the combustion zone and then dividing this distance by the velocity behind the normal shock wave. The velocity was calculated from the following normal shock relationships:

$$M_2^2 = \frac{(\gamma-1)M_1^2 + 2}{2\gamma M_1^2 - (\gamma-1)}$$

and

$$V_2 = M_2 \sqrt{\gamma R T_2}$$

where

$$T_2 = T_1 \left( 1 + \frac{\gamma-1}{2} M_1^2 \right)^{-1}$$

$M_1$  was assumed constant at the measured value of 3.1,  $\gamma$  was calculated from the ratio of specific heats of the mixture of  $O_2$ ,  $N_2$ ,  $H_2O$ , and  $H_2$  entering the shock wave at the total temperature, and  $R$  was the average gas constant of the mixture entering the shock.

Figure 12a shows the ignition time delay in microseconds times the oxygen concentration in gram moles per cubic centimeter plotted as a function of the reciprocal of the static temperature behind the shock. This parameter was chosen so that the data would be directly comparable with those of Nicholls (Ref. 2). They fall nearly in a straight line



roughly parallel to the theoretical curve, but a given temperature resulted in only about five percent of the delay predicted by theory.

The effect of temperature on time delay, without the correction for oxygen concentration, is shown in Fig. 12b for both the data from the SCT and those reported by Nicholls (Ref. 2). The time delays calculated from data taken in the SCT average about one third those reported by Nicholls.

These experimental ignition delay data are subject to some uncertainty because the distance between the shock wave and the apparent start of the emission is somewhat dependent on film exposure time. The emission seems to build up gradually downstream of the shock wave, and with longer exposures, the film records it closer to the shock.

#### CONCLUDING REMARKS

A series of tests was performed using the supersonic combustion tunnel in an attempt to understand the differences in the phenomena reported by Dr. R. A. Gross (at the Fairchild Engine Research Laboratory) using this tunnel and by Dr. J. A. Nicholls (at the University of Michigan) using an underexpanded free-jet nozzle when they attempted to burn hydrogen behind a normal shock wave.

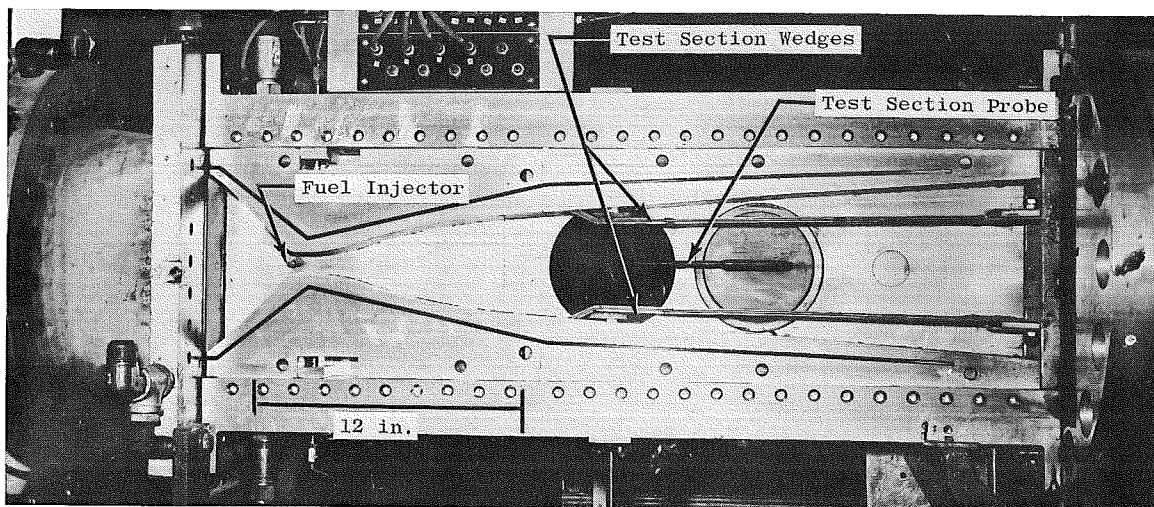
Those tests were performed using two different fuel injector configurations. In the first case, hydrogen was introduced upstream of the tunnel throat where the Mach number was about 0.6. The data indicated that this hydrogen started burning near the throat of the tunnel, and there was no evidence to indicate that the reaction was not essentially completed upstream of the normal shock in the test section. The "hysteresis effect", in which the fuel would burn at a temperature less than that required to ignite it, which was unexplained when it was thought that the reaction took place across the normal shock, becomes expected when the hydrogen is burning in a subsonic wake of the fuel injector. Also the forward motion of the normal shock when the fuel burns is explained by the reduction in Mach number of the core of the stream as a result of heat addition in the throat.

With a second hydrogen injector which introduced the fuel just downstream of the throat, there was no evidence of burning upstream of the normal shock in the test section. There was no "hysteresis" with this injector and no detectable change in the position of the normal shock as a function of fuel flow.

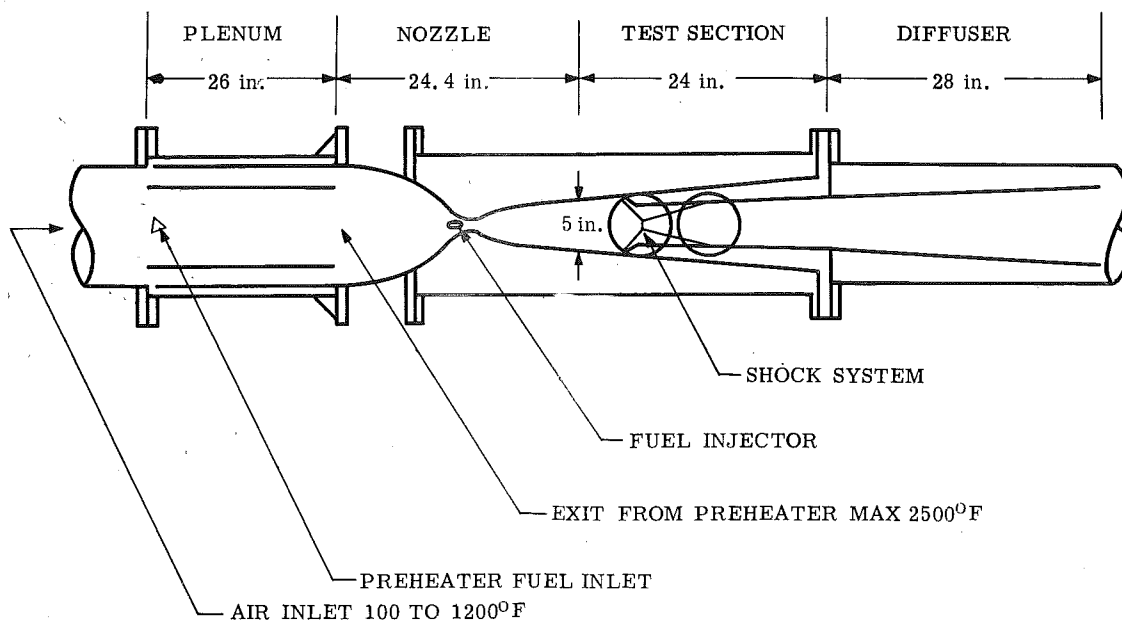
When sodium in the form of sodium hydroxide, was added to the hydrogen, emission from a reaction could be seen behind the normal shock when the static temperature in the flow behind the normal shock exceeded 1750°R. A delay was measured between the normal shock and the start of emission from the reaction which was an exponential function of the reciprocal of the temperature behind the shock wave.

#### REFERENCES

1. Gross, R. A. "Exploratory Studies of Combustion in Supersonic Flow." AFOSR TN 59-587, June 1959.
2. Nicholls, J. A. "Stabilization of Gaseous Detonation Waves with Emphasis on the Ignition Time Delay Zone." AFOSR TN 60-442, June 1960.
3. Rubins, P. M. "Installation and Calibration of a Supersonic Combustion Tunnel." AEDC-TN-60-162, September 1960.



a. Photograph



b. Schematic

Fig. 1 Supersonic Combustion Tunnel

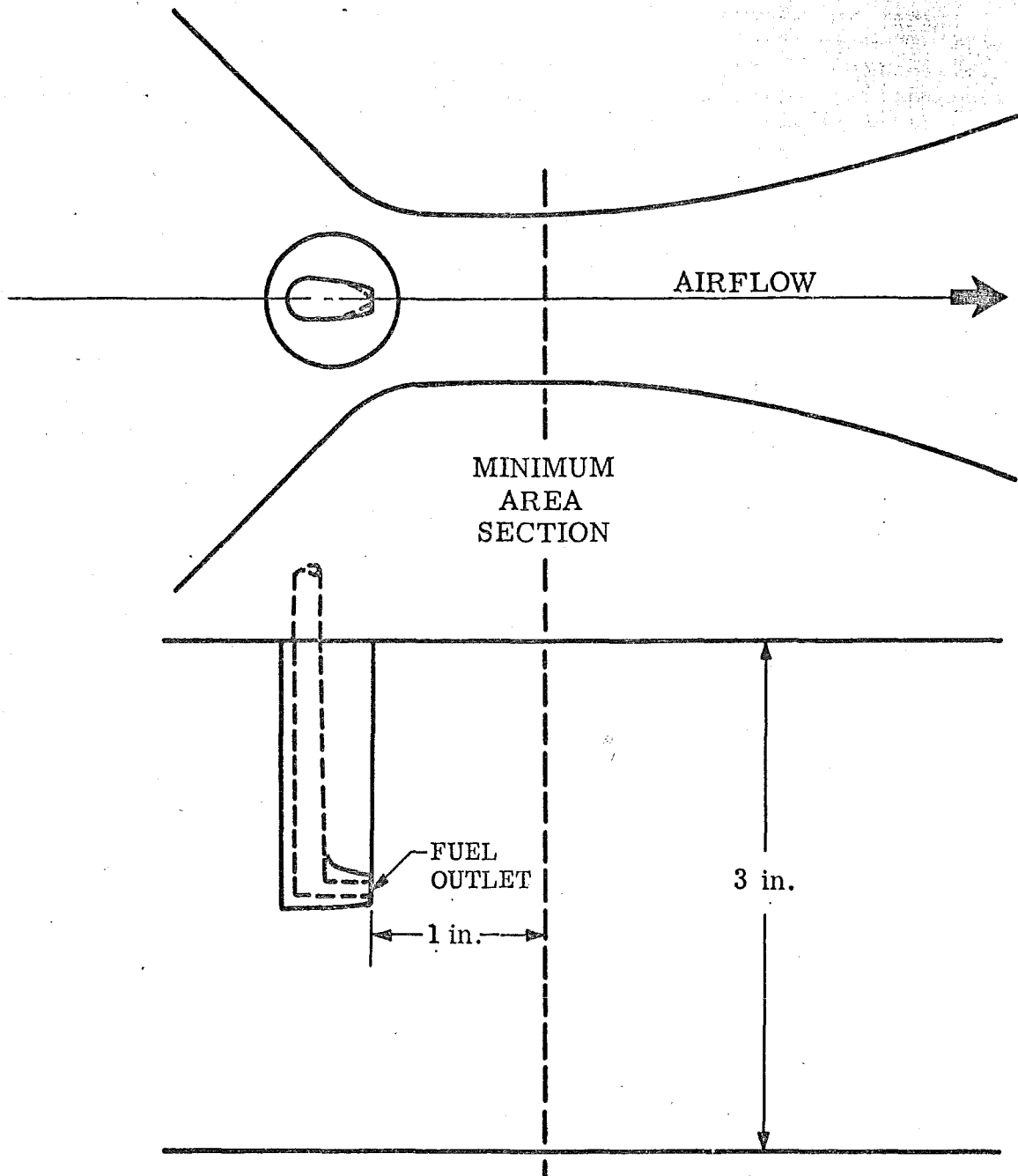


Fig. 2 Upstream Fuel Injector Installation

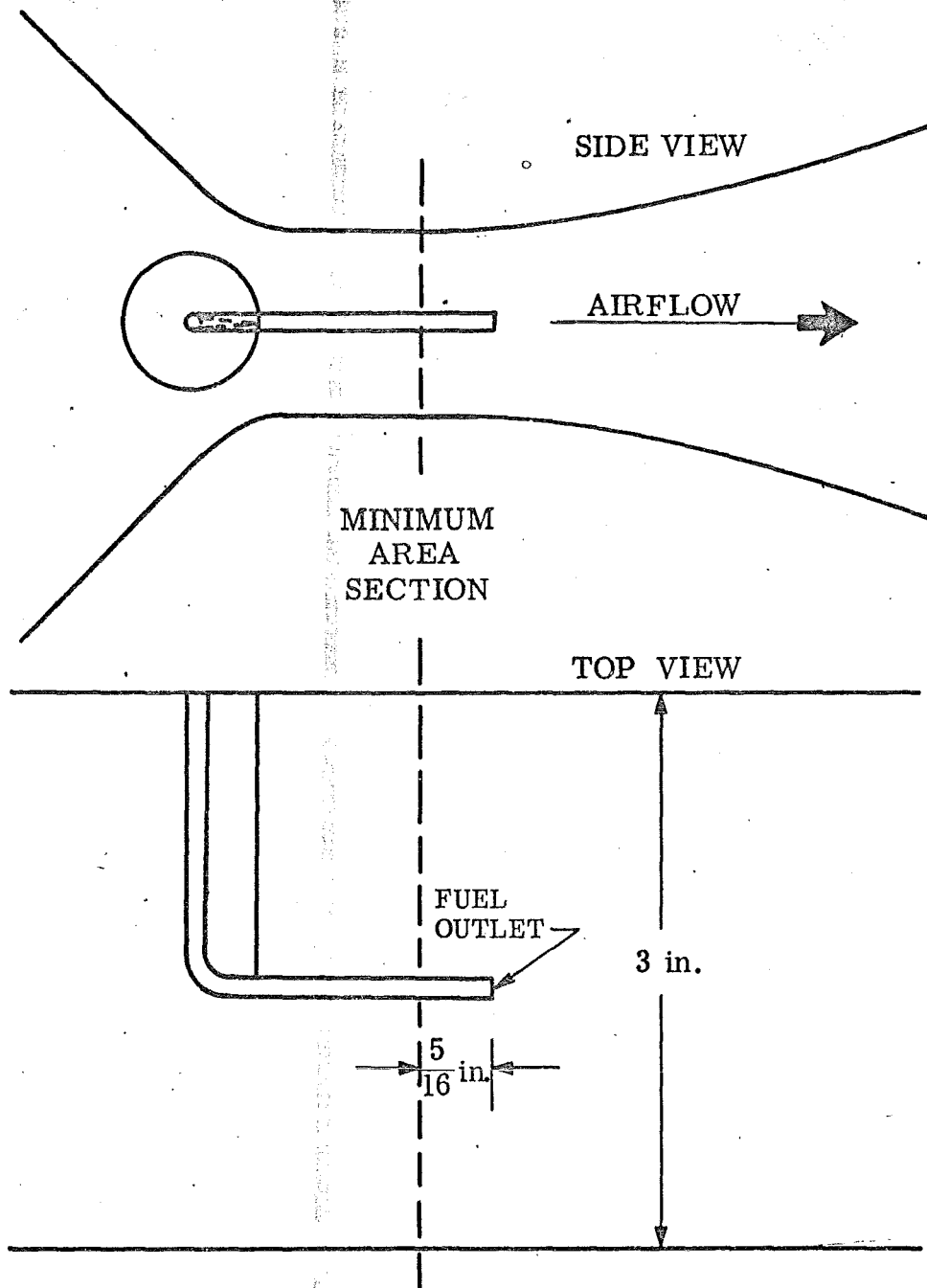


Fig. 3 Throat Fuel Injector Installation

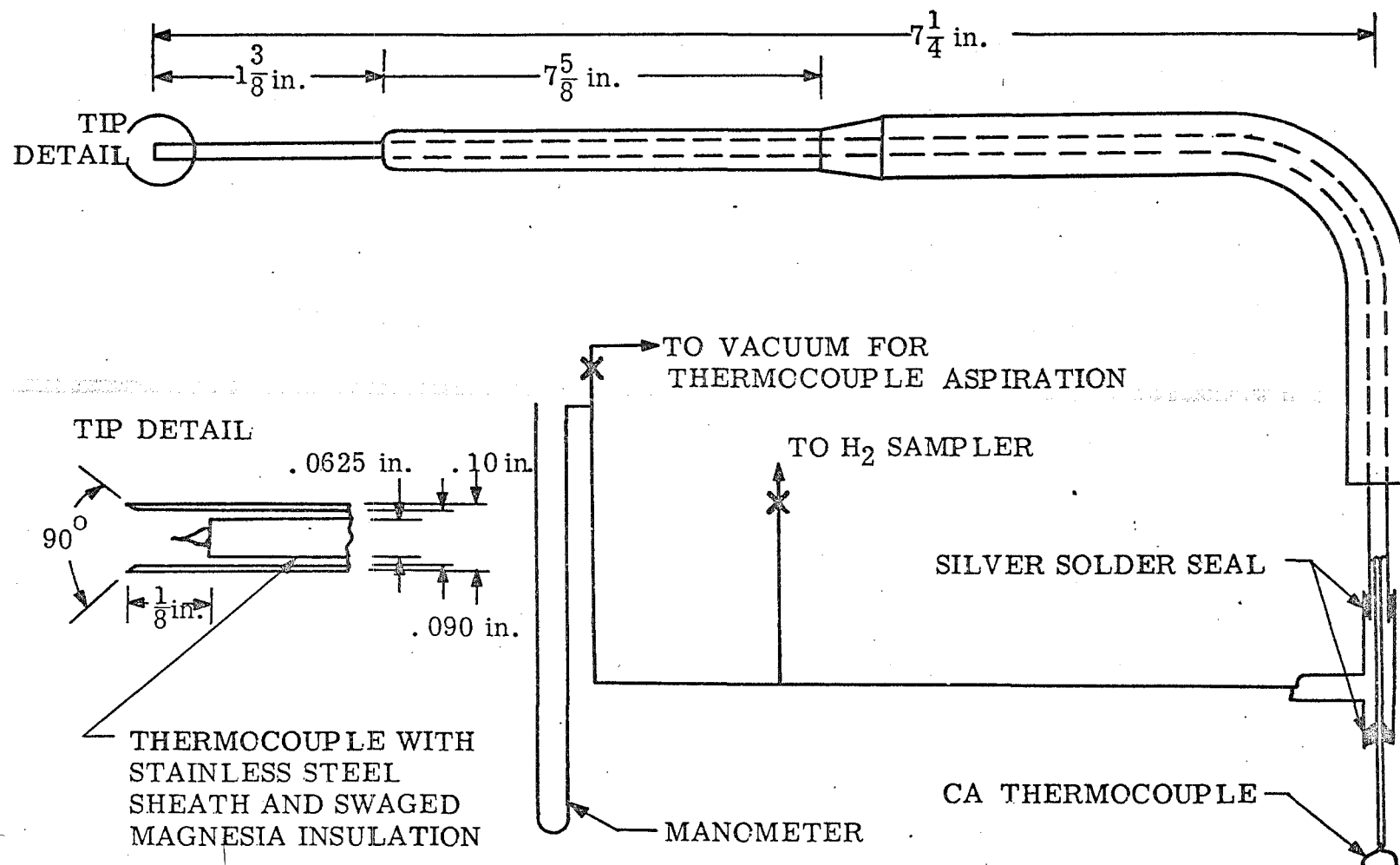


Fig. 4 Test Section Temperature, Pressure, and Sampling Probe Design

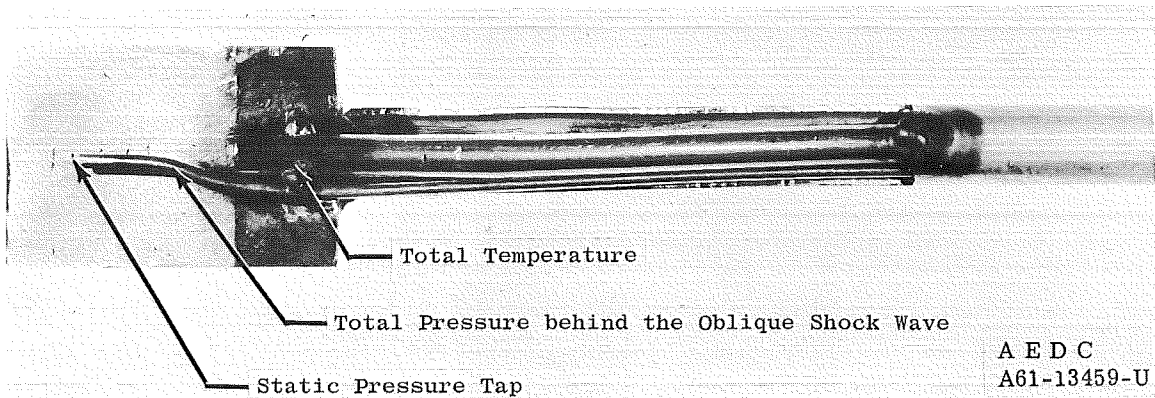
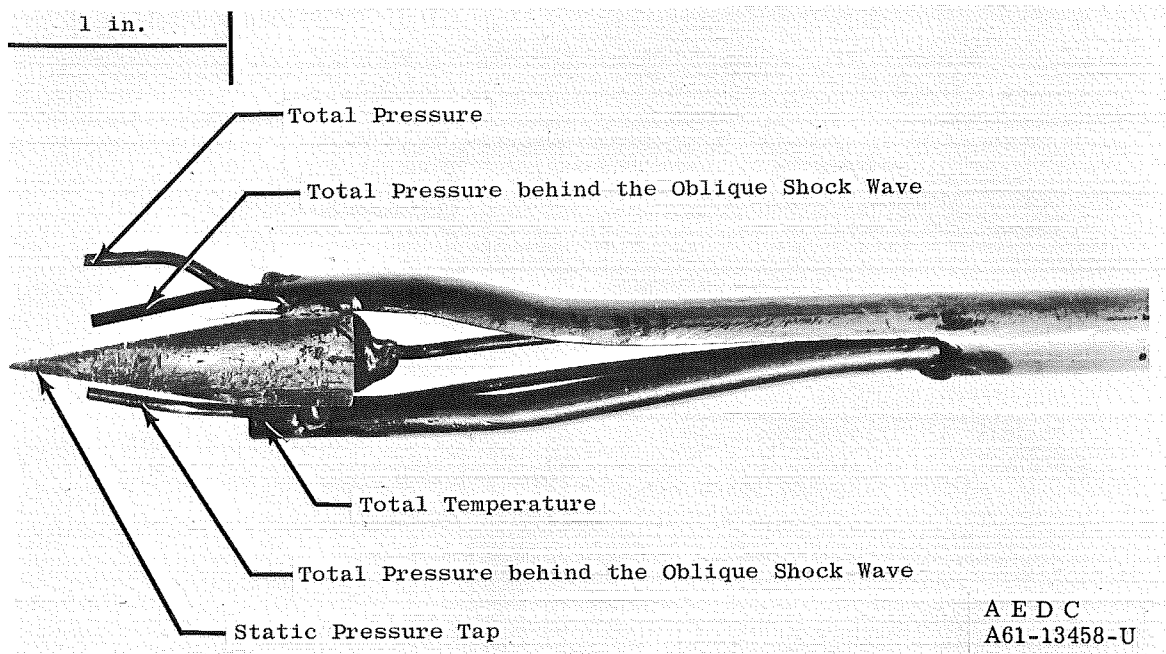


Fig. 5 Wedge-Type Pressure Probe

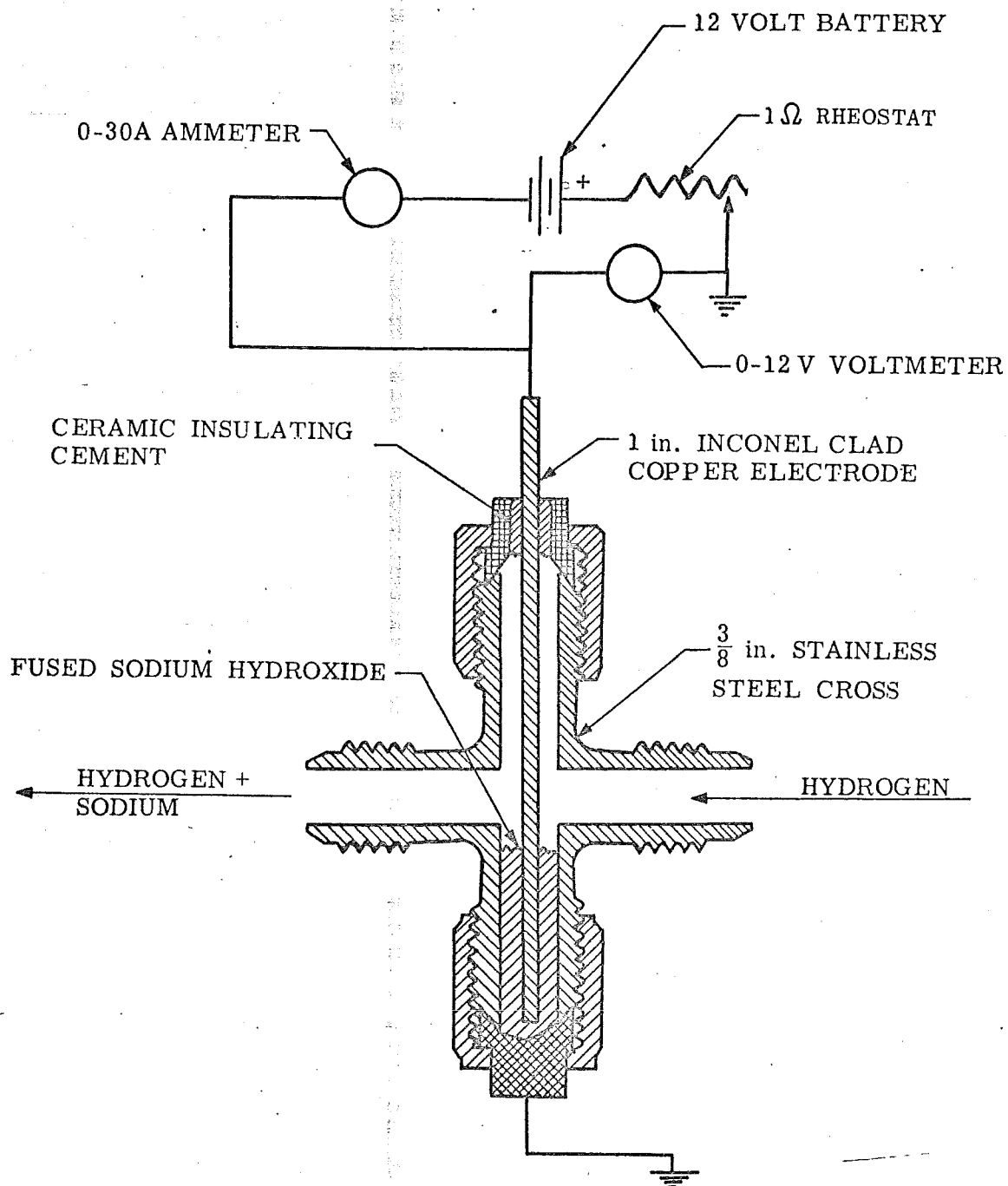


Fig. 6 Sodium Hydroxide Vaporizer



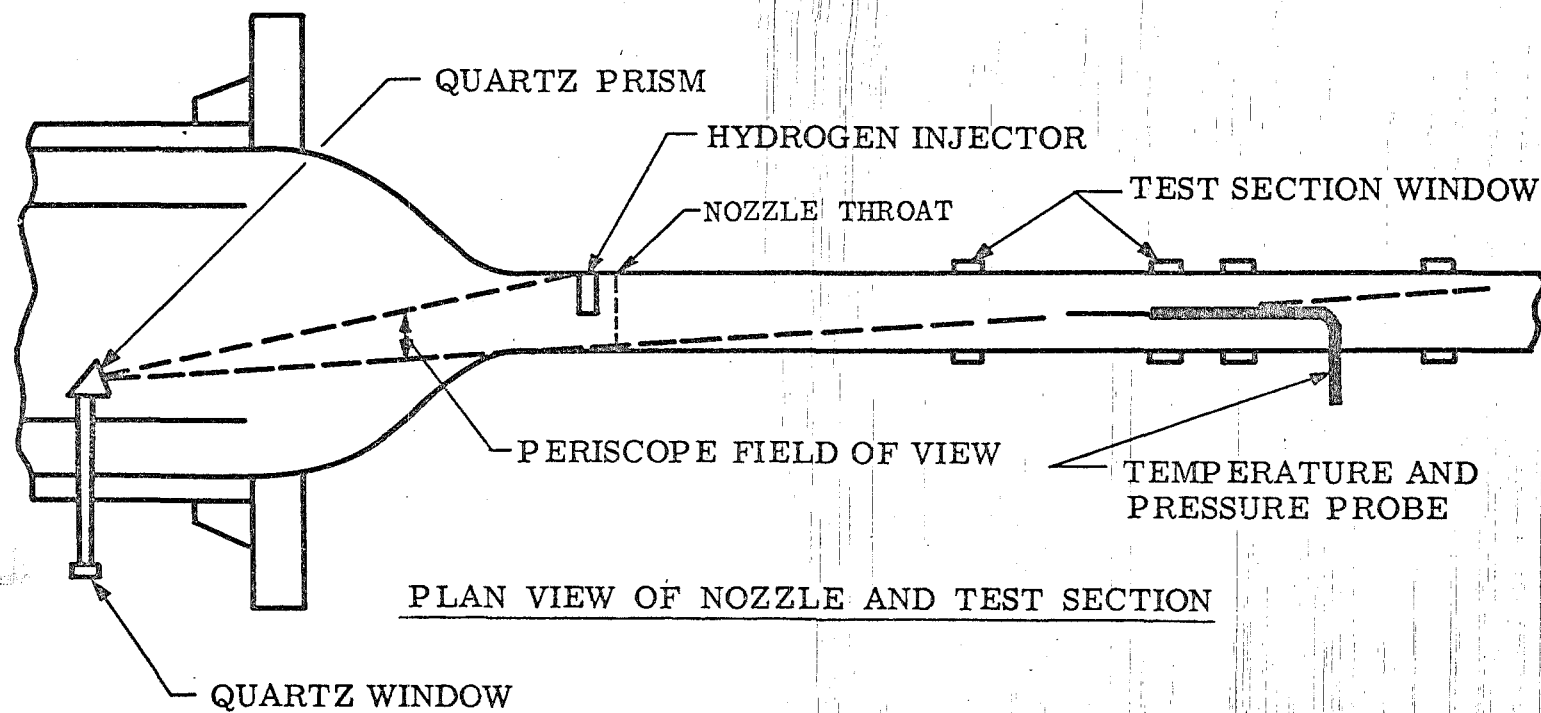


Fig. 7 Plenum Periscope Installation

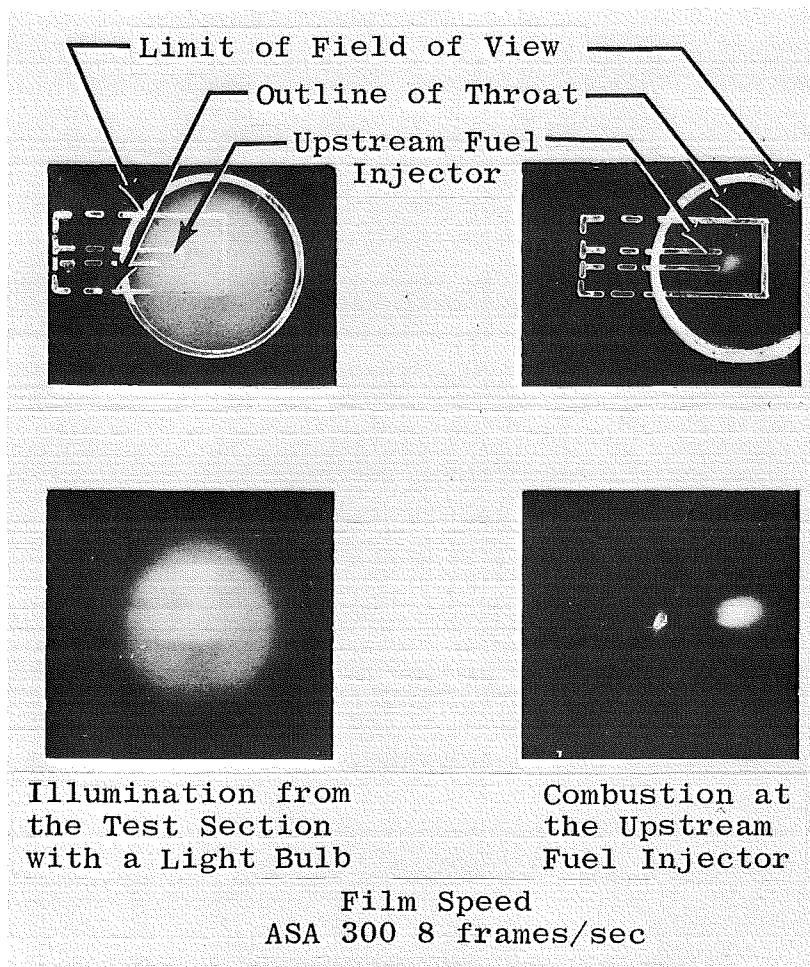
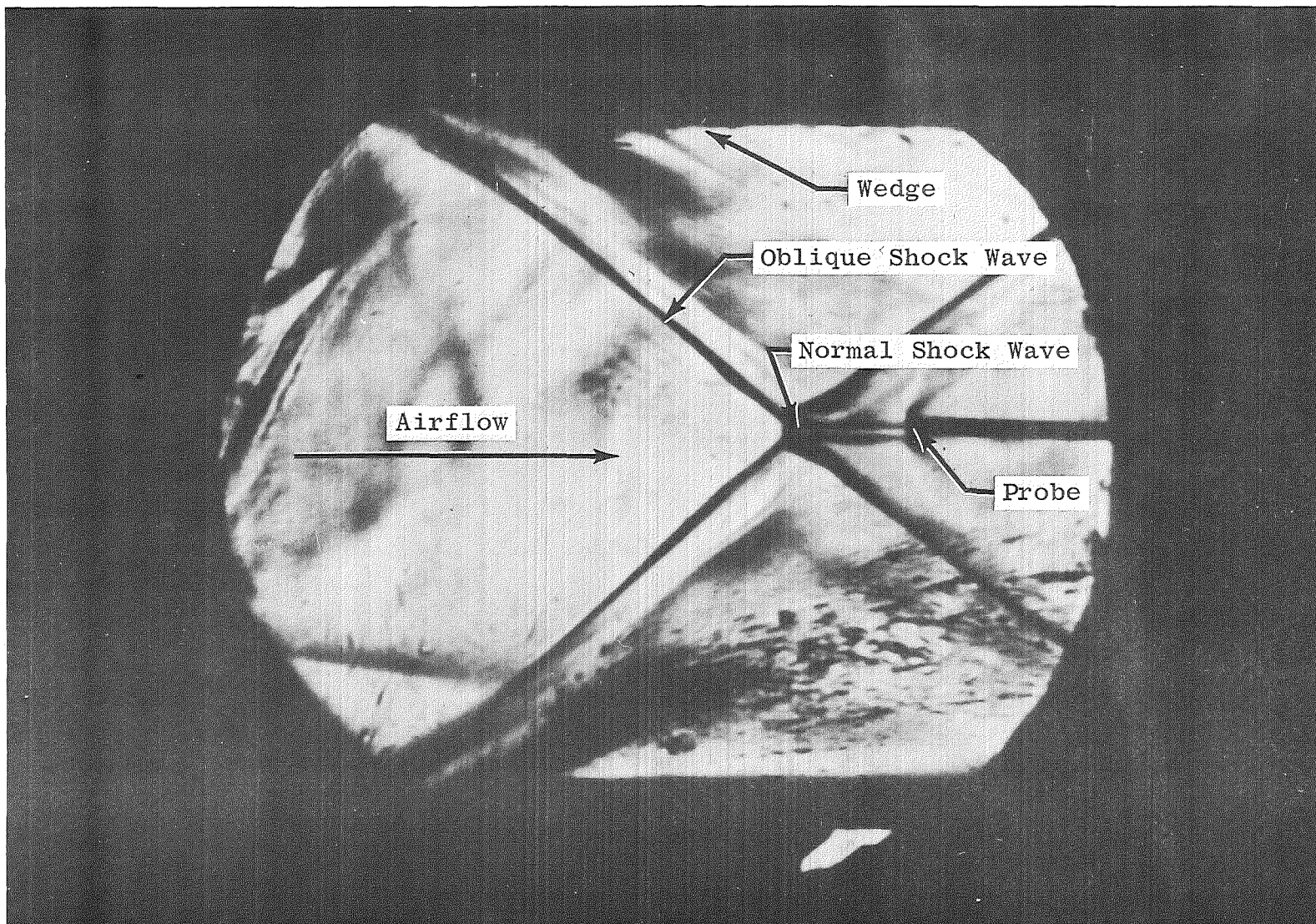
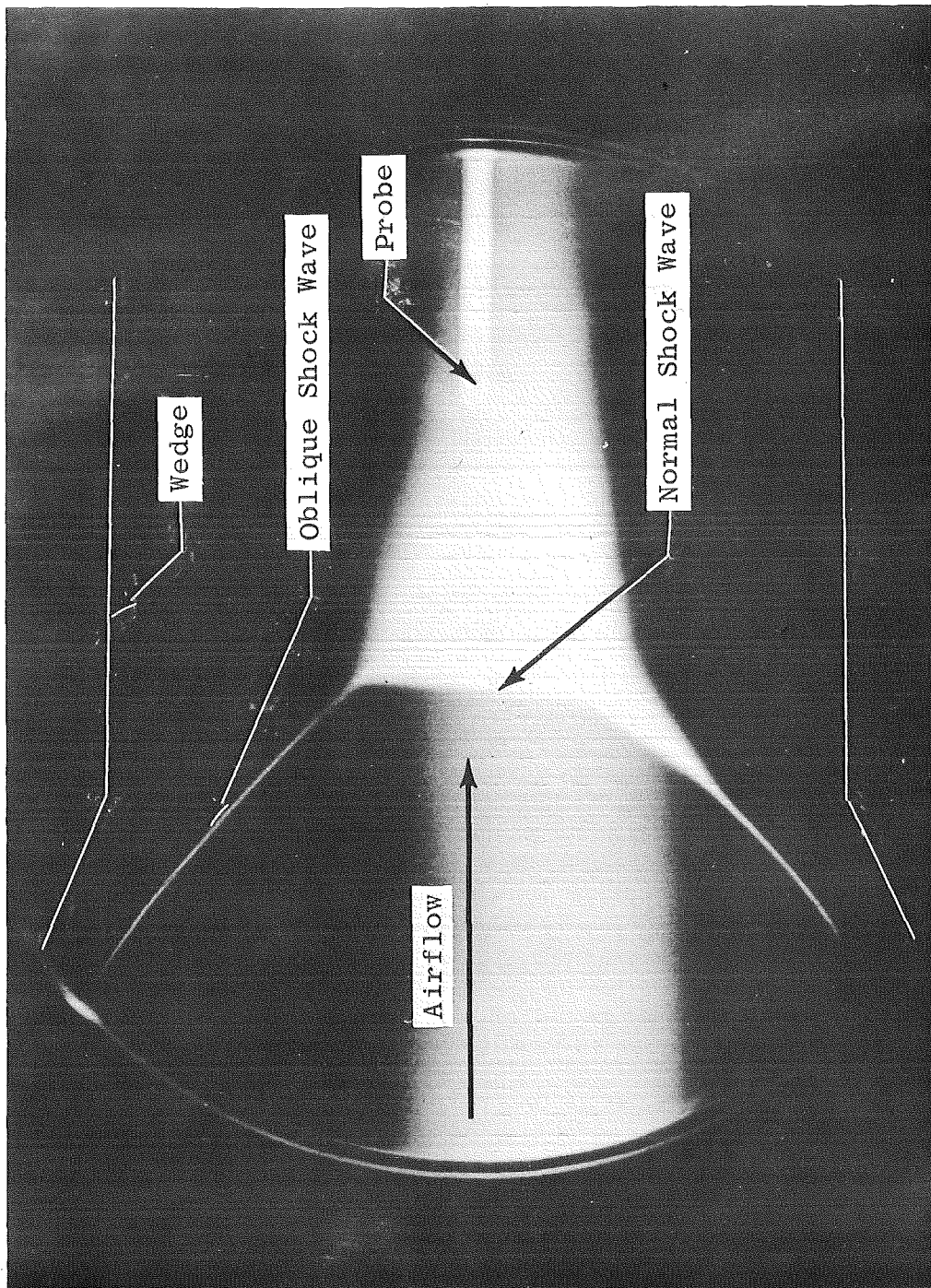


Fig. 8 Typical Views through the Plenum Periscope



a. No Fuel Injection, No Reaction,  $T_{T0} = 1460^{\circ}\text{R}$

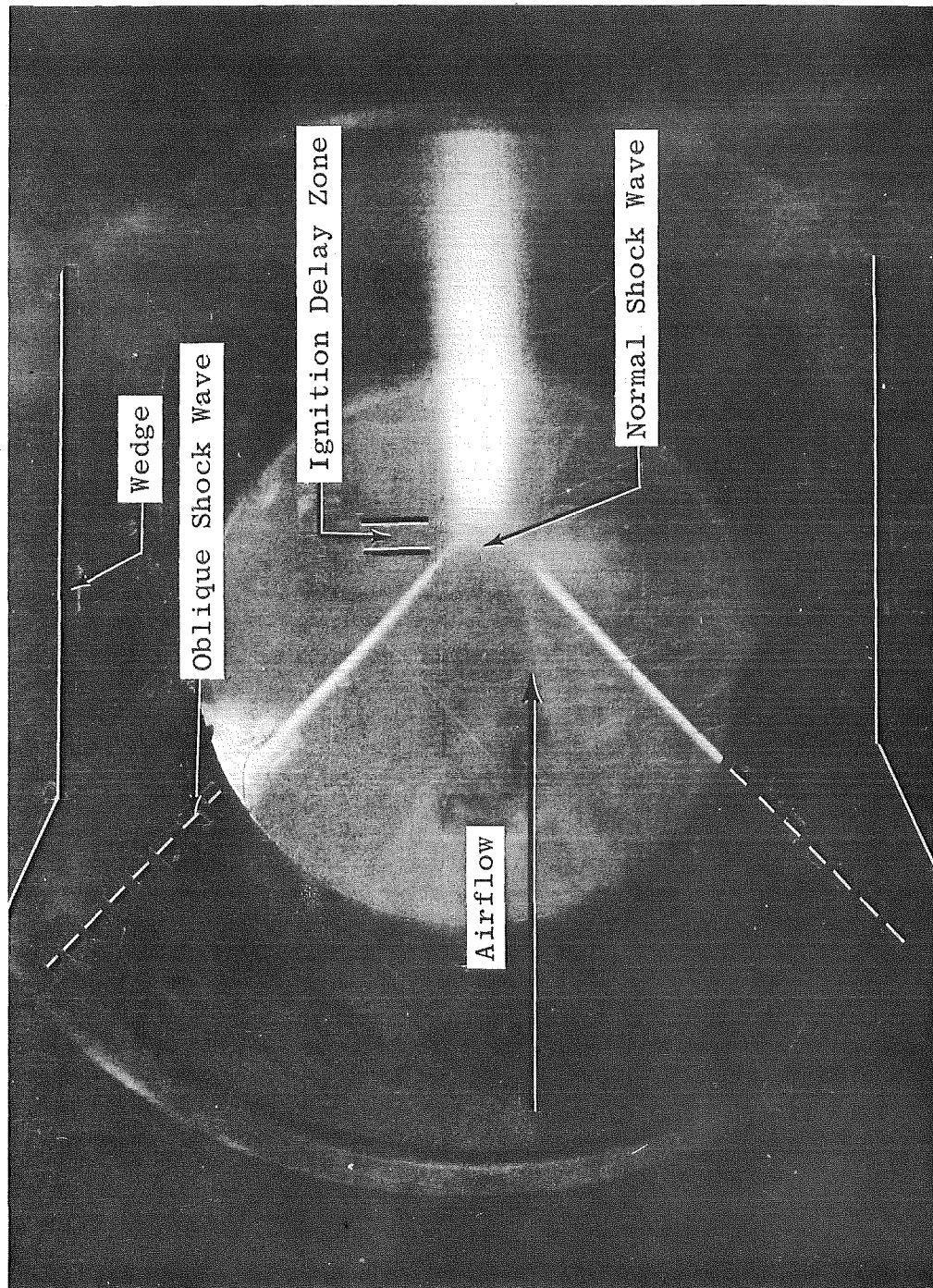
Fig. 9 Test Section Schlieren Photograph



b. Emission with Upstream Injector,  $T_{T0} = 1460^\circ\text{R}$ , Maximum  $\text{H}_2$  Concentration 0.08 mole  $\text{H}_2$ /mole Air

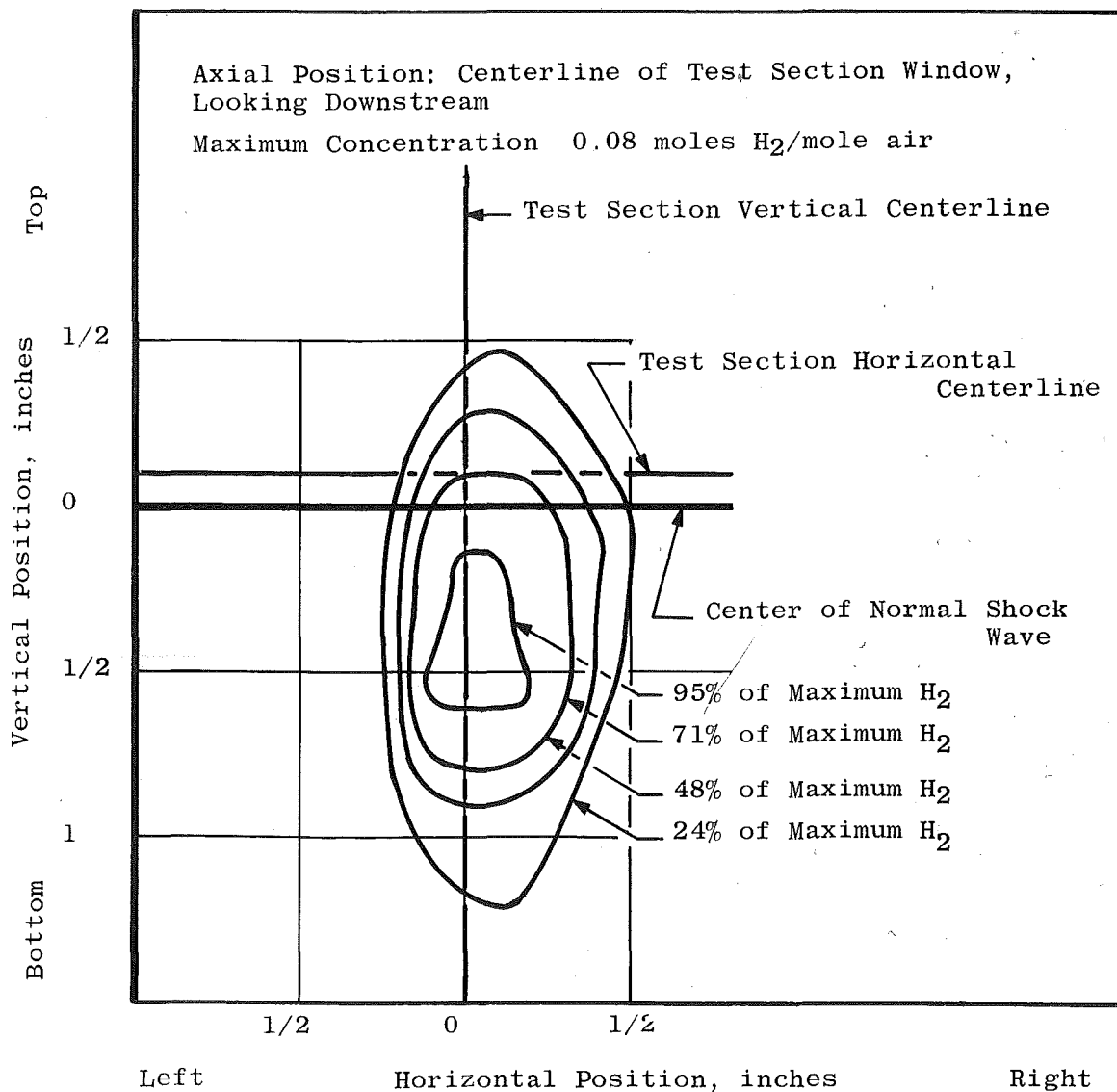
Fig. 9 Continued





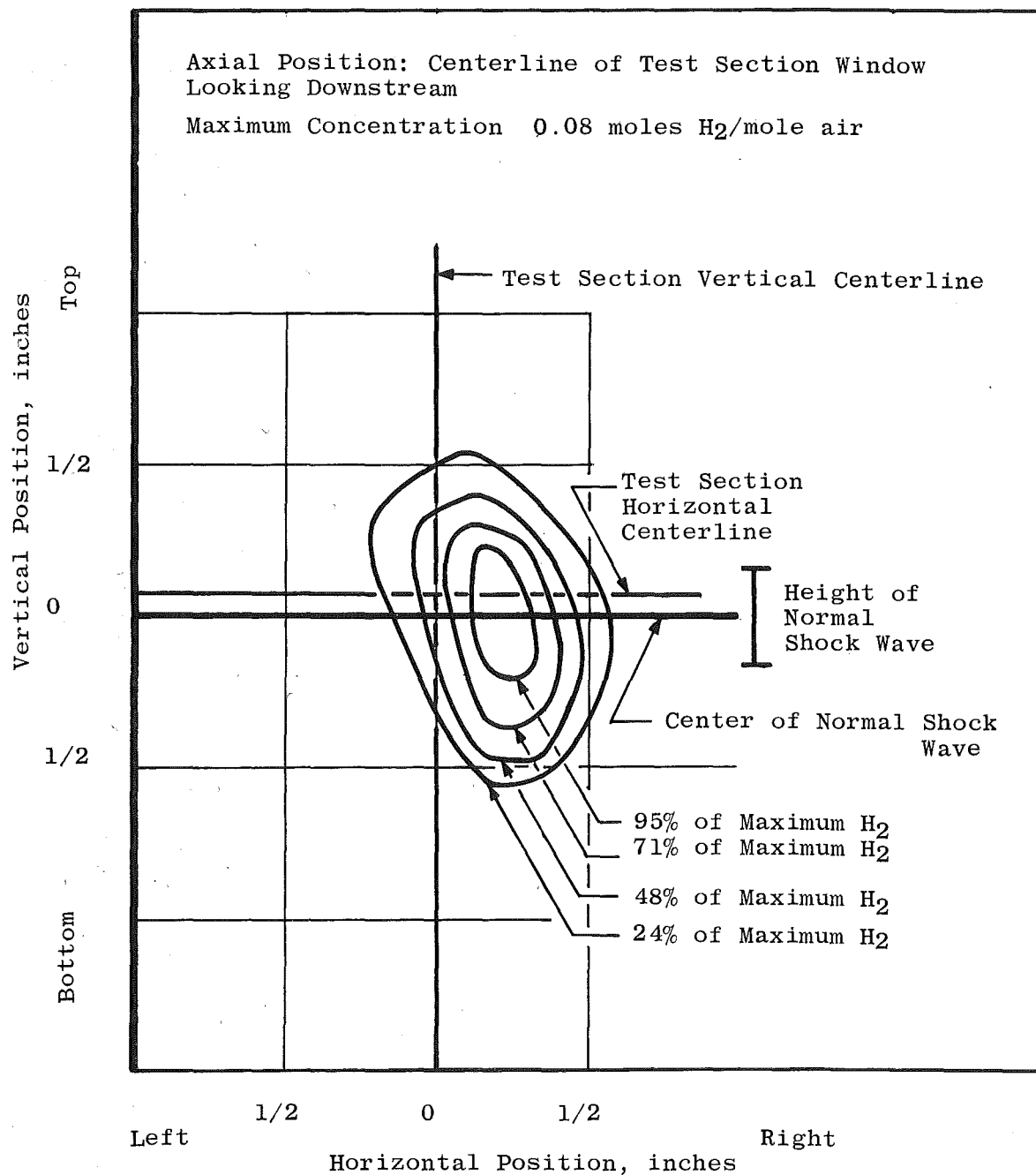
c. Emission with Throat Injection,  $T_{T0} = 2000^\circ\text{R}$ , Maximum  $\text{H}_2$  Concentration 0.08 mole  $\text{H}_2/\text{mole Air}$

Fig. 9 Concluded



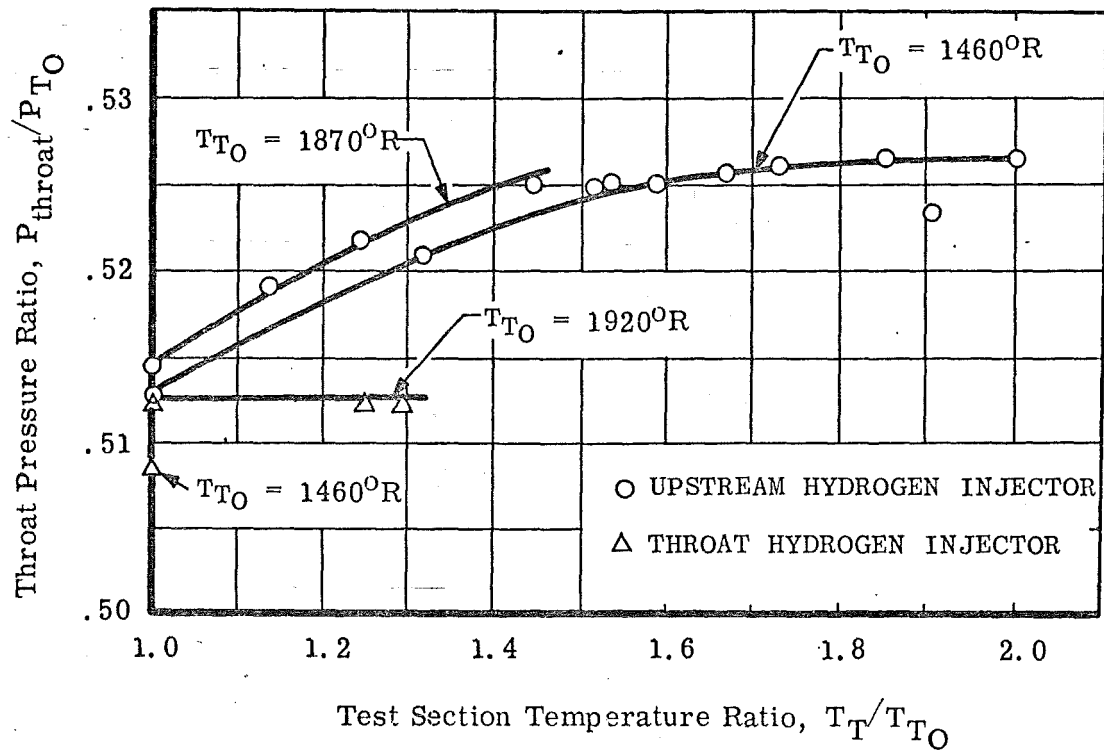
a. Upstream Fuel Injector

Fig. 10 Test Section Hydrogen Concentration



b. Throat Fuel Injector

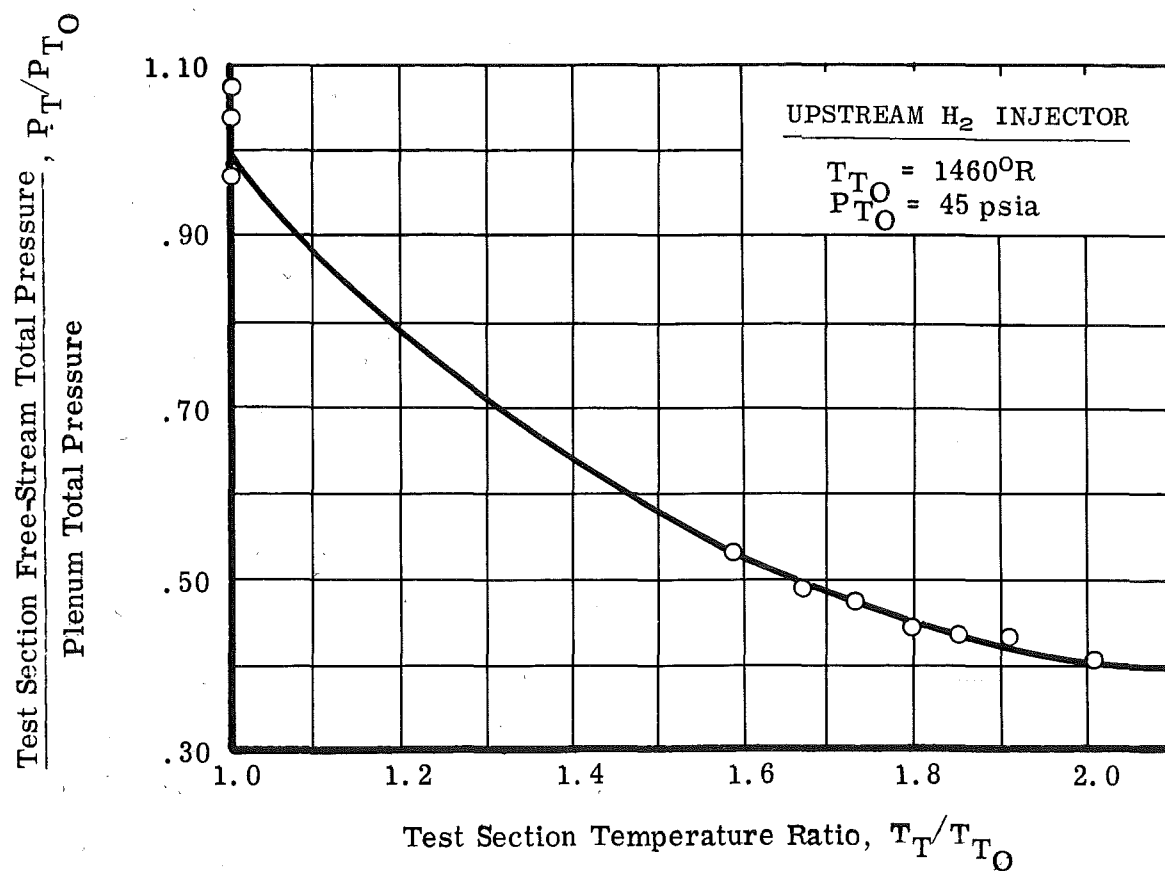
Fig. 10 Concluded



a. On Tunnel Throat Pressure Ratio

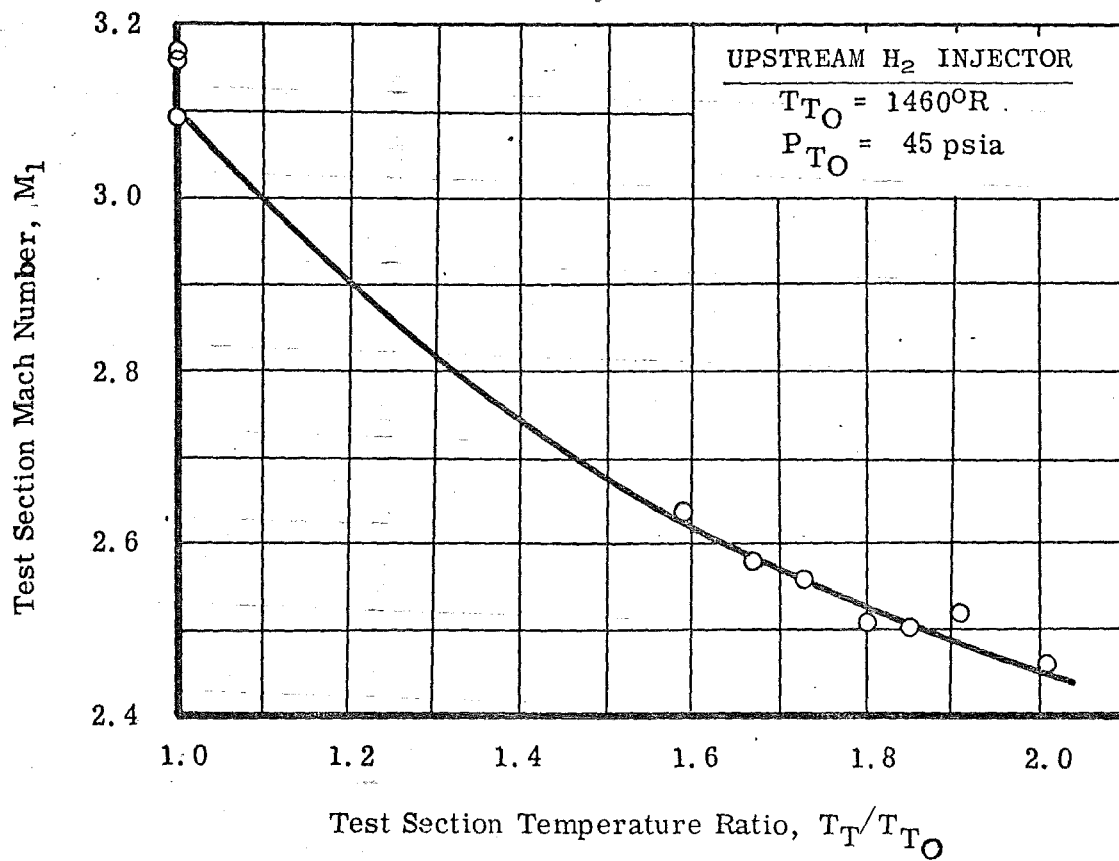
Fig. 11 Effect of Test Section Centerline Total Temperature Ratio from Burning Hydrogen





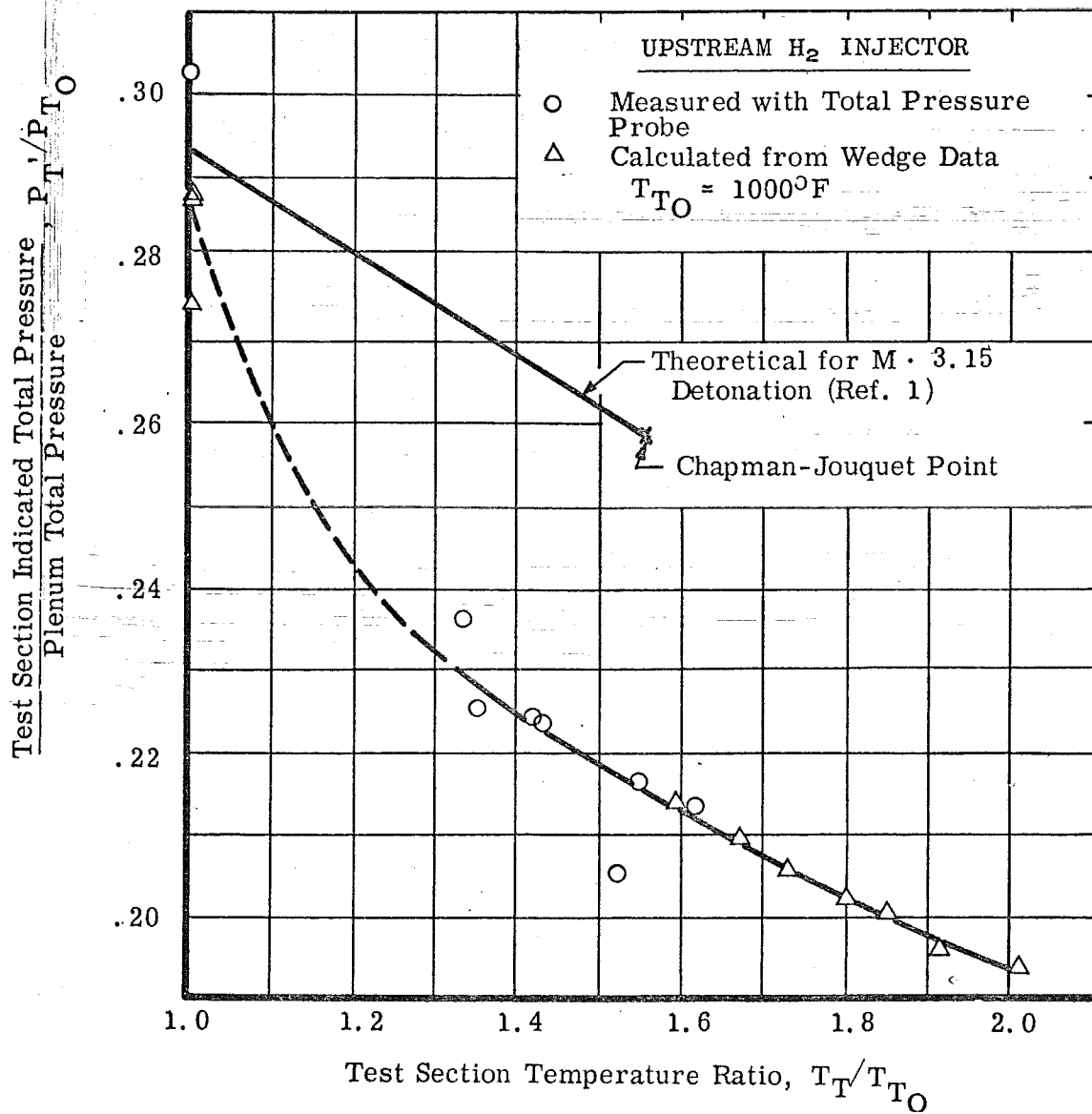
b. On Test Section Centerline Free-Stream Total Pressure Ratio

Fig. 11 Continued



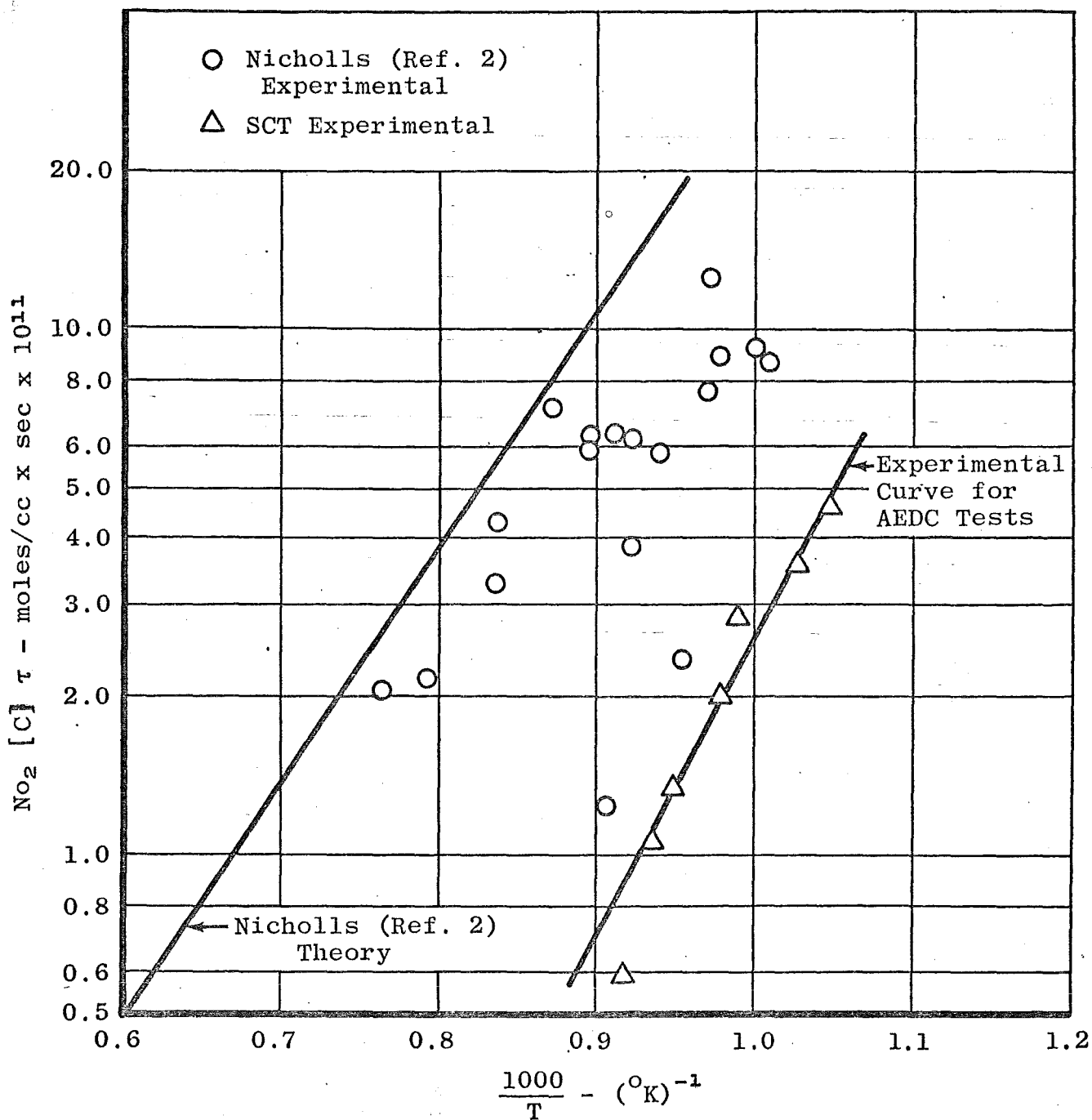
c. On Test Section Centerline Free-Stream Mach Number

Fig. 10 Continued



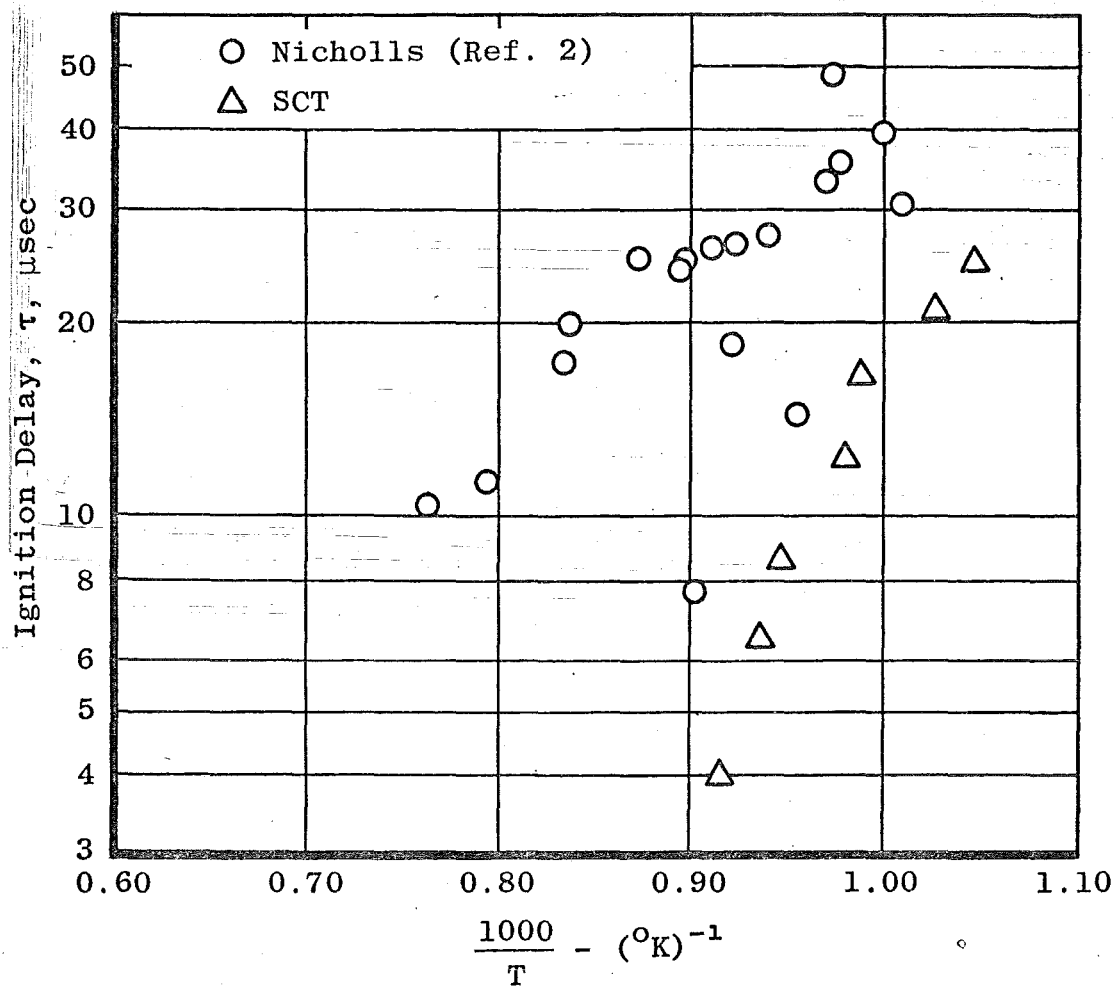
d. On Test Section Centerline Indicated Total Pressure Ratio

Fig. 11 Concluded



a. As a Function of Temperature and Oxygen Concentration

Fig. 12 Ignition Delay in the SCT



b. As a Function of Temperature

Fig. 12 Concluded